

The gamma-ray Doppler factor determinations for a Fermi blazar sample *

Jun-Hui Fan^{1,2}, Jiang-He Yang³, Yi Liu^{1,2} and Jing-Yi Zhang^{1,2}

¹ Center for Astrophysics, Guangzhou University, Guangzhou 510006, China;
jhfan_cn@yahoo.com.cn

² Astronomy Science and Technology Research Laboratory of Department of Education of Guangdong Province, Guangzhou 510006, China

³ Department of Physics and Electronics Science, Hunan University of Arts and Science, Changde 415000, China

Received 2012 October 12; accepted 2012 October 30

Abstract Observations suggest that γ -ray loud blazars are strongly beamed. The Fermi mission has detected many of blazars, which provide us with a good opportunity to investigate the emission mechanism and the beaming effect in the γ -ray region. We compiled the X-ray observations for 138 Fermi blazars (54 flat spectrum radio quasars, 36 low-peaked BL Lacertae objects, and 48 high-peaked BL Lacertae objects) and calculated their Doppler factors, δ_γ . It is interesting that the calculated Doppler factors, δ_γ , are strongly correlated with the γ -ray luminosity.

Key words: galaxies: active — galaxies: BL Lacertae objects — galaxies: quasars — galaxies: jets

1 INTRODUCTION

Blazars are an extreme subclass of active galactic nuclei (AGNs), that show rapid and large variability, high and variable polarization, superluminal motions in their radio components, and strong γ -ray emissions, etc (see Abdo et al. 2009, 2010; Ackermann et al. 2011; Aller et al. 2011; Bastieri et al. 2011; Fan et al. 1996, 2011; Ghisellini et al. 2010; Gupta 2011; Marscher et al. 2011; Nolan et al. 2012; Romero et al. 2002; Wills et al. 1992; Urry 2011). There are two subclasses of blazars, namely flat spectrum radio quasars (FSRQs) and BL Lacertae objects (BLs) with the former showing strong emission line features and the latter showing very weak emission lines or no emission lines at all. BL Lacertae objects are also divided into high-peaked BL Lacertae objects (HBLs) and low-peaked BL Lacertae objects (LBLs) (see Urry & Padovani 1995), and they were found to form a continuous sequence of objects with the discovery of the intermediate type of BL Lacertae objects (IBLs) (Nieppola et al. 2006; Lott 2010).

From the γ -ray emissions detected by the EGRET spacecraft, it is believed that the γ -ray emissions are strongly beamed, and a relativistic beaming effect was investigated for the γ -ray loud blazars from the correlations between the γ -ray emissions and the radio emissions (see Dondi &

* Supported by the National Natural Science Foundation of China.

Ghisellini 1995; Fan et al. 1998; Huang et al. 1999). The γ -ray Doppler factors have even been estimated for some γ -ray loud blazars. For example, for the quasar 1633+382, $\delta_\gamma = 7.6$, and for 3C 279, $\delta_\gamma = 3.9 \sim 5.2$ (Mattox et al. 1993; von Montigny et al. 1995). We also discussed the estimation of the γ -ray Doppler factors for some γ -ray loud blazars (Fan et al. 1999; Fan 2005).

Since the launch of the new generation Fermi γ -ray detector, it has recorded many blazars (see Abdo et al. 2010; Ackermann et al. 2011; Nolan et al. 2012). The relativistic beaming effect has been discussed for blazars observed by Fermi (see Kovalev et al. 2009; Arshakian et al. 2010; Savolainen et al. 2010; and Pushkarev et al. 2010), but the γ -ray Doppler factors have not been estimated for those blazars. It is known that the Doppler factors are important in the discussion of blazars, therefore, we will estimate the factors for those Fermi detected blazars with available X-ray emission data. In Section 2, we will show the sample and the results; in Section 3, we will give some discussions and a brief conclusion. We adopt $H_0 = 73 \text{ km s}^{-1} \text{ Mpc}^{-1}$, and the spectral index, α , is defined as $f_\nu \propto \nu^{-\alpha}$ throughout this paper.

2 SAMPLE AND RESULTS

2.1 Pair-Production Optical Depth

The extreme observation properties of blazars, such as rapid variability, high and variable polarization, and superluminal motion, can be explained using a relativistic beaming model. The strong γ -rays detected from blazars imply that the beaming effect is presented in those sources, otherwise the γ -rays should have been absorbed due to pair-production when collision occurs with photons of lower energy. In 1993, Mattox et al. considered the pair-production optical depth. They assumed that (1) the X-ray is produced in the same region as the γ -rays, and that a similar X-ray intensity was extant at the time of the γ -ray observation; (2) the emission region is spherical; (3) the emission is isotropic, and the size of the emission region is constrained by time variation to be less than $R = c\Delta T/(1+z)$, where ΔT is the timescale of variability, c is the speed of light, and z is the redshift. Finally, they obtained the optical depth,

$$\tau = 2 \times 10^3 \left[(1+z)/\delta \right]^{(4+2\alpha)} \left(1 + z - \sqrt{1+z} \right)^2 h_{75}^{-2} \Delta T_5^{-1} \times \frac{F_{\text{keV}}}{\mu\text{Jy}} \left(\frac{E_\gamma}{\text{GeV}} \right)^\alpha, \quad (1)$$

where δ is the Doppler factor, α is the X-ray spectral index ($F_{\nu_X} \propto \nu_X^{-\alpha}$), $h_{75} = H_0/75$, $\Delta T_5 = \Delta T/(10^5 \text{ s})$, F_{keV} is the flux density at 1 keV and E_γ is the energy at which the γ -rays are detected. If we use a Λ -CDM model (Capelo & Natarajan 2007) for the luminosity distance,

$$d_L = \frac{c}{H_0} \int_1^{1+z} \frac{1}{\sqrt{\Omega_M x^3 + 1 - \Omega_M}} dx \quad (2)$$

with $\Omega_\Lambda \simeq 0.7$, $\Omega_M \simeq 0.3$ and $\Omega_K \simeq 0.0$, then the optical depth can be rewritten as

$$\tau = 1.54 \times 10^{-3} \left(\frac{1+z}{\delta} \right)^{4+2\alpha} \left(\frac{d_L}{\text{Mpc}} \right)^2 \left(\frac{\Delta T}{\text{h}} \right)^{-1} \left(\frac{F_{\text{keV}}}{\mu\text{Jy}} \right) \left(\frac{E_\gamma}{\text{GeV}} \right)^\alpha. \quad (3)$$

So, the lower limit of the Doppler factor can be estimated if we assume that the optical depth does not exceed unity (see Fan et al. 2012a).

$$\delta \geq \left[1.54 \times 10^{-3} (1+z)^{4+2\alpha} \left(\frac{d_L}{\text{Mpc}} \right)^2 \left(\frac{\Delta T}{\text{h}} \right)^{-1} \left(\frac{F_{\text{keV}}}{\mu\text{Jy}} \right) \left(\frac{E_\gamma}{\text{GeV}} \right)^\alpha \right]^{\frac{1}{4+2\alpha}}. \quad (4)$$

2.2 Sample

Based on the second catalog of Fermi gamma-ray LAT (2FGL) (Ackermann et al. 2011; Nolan et al. 2012), we compiled the available X-ray data from the literature and listed them in Table 1.

Table 1 γ -ray Doppler Factor for Fermi Blazars

Name (1)	Other name (2)	C (3)	z (4)	F_γ (5)	α_γ (6)	$F_{1\text{ keV}}$ (7)	α_X (8)	Ref (9)	E_γ (10)	δ_γ (11)	$\log L_\gamma$ (12)
2FGLJ0035.8+5951	1ES 0033+595	H	0.086	2.43E-09	1.87	5.66	1.84	NED	5.59	2.74	44.56
2FGLJ0050.6-0929	PKS 0048-09	L	0.634	3.85E-09	2.14	0.77	1.57	D01	3.89	5.47	46.61
2FGLJ0109.0+1817	BZB J0109+1816	H	0.145	5.00E-10	1.992	1.18	0.94	D01	4.7	2.65	44.29
2FGLJ0112.1+2245	S2 0109+22	L	0.265	7.13E-09	2.066	0.16	1.96	D01	4.26	2.59	46.00
2FGLJ0115.7+2518	RX J0115.7+2519	H	0.35	1.29E-09	1.998	0.71	0.84	D01	4.66	4.08	45.57
2FGLJ0120.4-2700	PKS 0118-272	L	0.559	4.35E-09	1.927	0.28	1.74	D01	5.15	4.56	46.61
2FGLJ0137.6-2430	PKS 0135-247	F	0.837	1.05E-09	2.423	0.535	0.18	NED	2.89	9.18	46.30
2FGLJ0141.5-0928	PKS 0139-09	L	0.733	1.64E-09	2.033	0.208	1.15	NED	4.45	5.50	46.44
2FGLJ0205.4+3211	B2 0202+31	F	1.466	4.80E-10	2.664	0.106	0.32	NED	2.39	10.87	46.64
2FGLJ0210.7-5102	PKS 0208-512	F	0.999	3.79E-09	2.395	0.61	1.04	D01	2.96	8.12	47.07
2FGLJ0217.7+7353	S5 0212+73	F	2.367	7.30E-10	2.824	0.26	-0.34	D01	2.16	42.59	47.47
2FGLJ0217.9+0143	PKS 0215+015	F	1.715	5.66E-09	2.152	0.258	0.37	NED	3.83	15.90	47.89
2FGLJ0222.6+4302	3C 66A	L	0.444	2.56E-08	1.847	1.56	1.6	D01	5.78	5.14	47.18
2FGLJ0238.7+1637	AO 0235+164	L	0.94	1.87E-08	2.023	1.15	1.59	D01	4.51	8.11	47.77
2FGLJ0303.4-2407	PKS 0301-243	L	0.26	6.73E-09	1.938	0.27	1.68	D01	5.07	2.87	46.02
2FGLJ0319.6+1849	RBS 0413	H	0.19	1.06E-09	1.551	2.05	1.08	D01	9.2	3.73	45.14
2FGLJ0326.1+0224	1H 0323+022	H	0.147	1.29E-09	2.056	3.21	1.27	D01	4.32	3.04	44.68
2FGLJ0334.2-4008	PKS 0332-403	F	1.445	4.33E-09	2.189	0.14	0.6	D01	3.67	10.60	47.58
2FGLJ0405.8-1309	PKS 0403-13	F	0.571	4.60E-10	2.347	0.4	0.78	D01	3.1	5.03	45.52
2FGLJ0407.3-3826	PKS 0405-385	F	1.285	2.01E-09	2.338	0.0521	0.07	NED	3.13	8.93	47.09
2FGLJ0416.8+0105	1ES 0414+009	H	0.287	6.90E-10	1.981	4.69	1.63	D01	4.77	4.42	45.10
2FGLJ0423.2-0120	PKS 0420-01	F	0.916	6.65E-09	2.298	0.28	0.86	D01	3.26	7.01	47.23
2FGLJ0428.6-3756	PKS 0426-380	L	1.11	3.11E-08	1.946	0.09	2.2	D01	5.01	6.38	48.19
2FGLJ0505.4+0419	BZB J0505+0415	H	0.027	7.60E-10	2.151	0.73	1.35	D01	3.84	1.25	42.86
2FGLJ0508.0+6737	1ES 0502+675	H	0.314	2.42E-09	1.489	8.51	1.34	D01	10.2	6.17	46.01
2FGLJ0530.8+1333	PKS 0528+134	F	2.06	2.57E-09	2.218	1.48	0.58	D01	3.55	24.91	47.75
2FGLJ0538.8-4405	PKS 0537-441	L	0.894	3.71E-08	2.012	0.78	1.04	D01	4.58	8.25	48.01
2FGLJ0539.3-2841	PKS 0537-286	F	3.104	6.10E-10	2.825	0.458	0.86	NED	2.16	26.07	47.75
2FGLJ0558.2-3837	EXO 0556.4-3838	H	0.302	7.00E-10	2.255	1.42	1.52	D01	3.41	3.62	45.05
2FGLJ0635.5-7516	PKS 0637-75	F	0.653	1.73E-09	2.648	0.49	0.64	D01	2.42	5.87	46.21
2FGLJ0641.2+7315	S5 0633+73	F	1.85	7.00E-10	2.4	0.0891	0.32	NED	2.95	13.91	47.07
2FGLJ0650.7+2505	1ES 0647+250	H	0.203	1.78E-09	1.595	6.01	1.47	D01	8.57	4.42	45.40
2FGLJ0710.5+5908	1H 0658+595	H	0.125	8.10E-10	1.534	1.83	1.15	D01	9.46	3.01	44.65
2FGLJ0721.9+7120	S5 0716+71	L	0.3	1.83E-08	2.007	2.98	1.77	D01	4.61	4.16	46.56
2FGLJ0738.0+1742	PKS 0735+17	L	0.424	5.16E-09	2.047	0.22	1.34	D01	4.37	3.63	46.35
2FGLJ0739.2+0138	PKS 0736+01	F	0.189	2.54E-09	2.229	0.64	0.76	D01	3.51	2.66	45.15
2FGLJ0745.0+7436	MS 0737.9+7441	H	0.315	6.30E-10	1.799	0.88	1.53	D01	6.21	3.94	45.25
2FGLJ0746.6+2549	B2 0743+25	F	2.979	5.80E-10	2.846	0.54	0.11	NED	2.14	43.19	47.68
2FGLJ0757.1+0957	PKS 0754+100	L	0.266	2.05E-09	2.192	0.72	1.11	D01	3.66	3.22	45.41
2FGLJ0808.2-0750	PKS 0805-07	F	1.837	1.50E-08	1.928	0.109	0.35	NED	5.14	14.81	48.42
2FGLJ0809.8+5218	1ES 0806+524	H	0.138	2.45E-09	1.938	4.91	1.93	D01	5.07	3.13	44.97
2FGLJ0811.4+0149	OJ 014	L	1.148	1.26E-09	2.262	0.38	0.92	D01	3.39	9.04	46.77
2FGLJ0818.2+4223	S4 0814+42	L	0.53	7.21E-09	2.142	0.05	0.16	D01	3.88	3.48	46.70
2FGLJ0831.9+0429	PKS 0829+046	L	0.174	5.00E-09	2.047	0.4	2.26	D01	4.37	2.42	45.44
2FGLJ0841.6+7052	4C +71.07	F	2.172	7.22E-10	2.948	1.6	0.42	D01	2.03	28.29	47.38
2FGLJ0847.2+1134	BZB J0847+1133	H	0.198	5.30E-10	1.483	1.98	1.5	D01	10.3	3.88	44.92
2FGLJ0854.8+2005	OJ 287	L	0.306	3.55E-09	2.232	0.93	1.5	D01	3.5	3.46	45.78
2FGLJ0920.9+4441	S4 0917+44	F	2.19	9.10E-09	2.109	0.47	0.39	D01	4.04	23.93	48.37
2FGLJ0957.7+5522	4C +55.17	F	0.896	1.12E-08	1.831	0.1	1.17	D01	5.92	6.09	47.56
2FGLJ0958.6+6533	S4 0954+65	L	0.368	1.36E-09	2.415	0.16	0.96	D01	2.91	3.00	45.50
2FGLJ1015.1+4925	1H 1013+498	H	0.212	7.80E-09	1.723	2.15	1.49	D01	6.99	3.73	46.01
2FGLJ1031.0+5053	1ES 1028+511	H	0.36	1.15E-09	1.815	2.55	1.44	D01	6.06	4.98	45.64
2FGLJ1033.2+4117	S4 1030+41	F	1.117	1.13E-09	2.444	0.0964	0.51	NED	2.84	7.52	46.67
2FGLJ1037.6+5712	GB6 J1037+5711	H	0.83	2.88E-09	1.906	0.38	1.42	D01	5.3	6.65	46.86
2FGLJ1042.6+8053	S5 1039+81	F	1.26	4.60E-10	2.54	0.18	0.83	D01	2.62	8.59	46.42
2FGLJ1048.3+7144	S5 1044+71	F	1.15	2.42E-09	2.342	0.129	0.18	NED	3.12	9.33	47.05
2FGLJ1053.6+4928	GB6 J1053+4930	H	0.14	9.20E-10	1.746	0.09	1.62	D01	6.74	1.97	44.68

Table 1 – Continued.

Name (1)	Other name (2)	C (3)	z (4)	F_{γ} (5)	α_{γ} (6)	$F_{1\text{ keV}}$ (7)	α_X (8)	Ref (9)	E_{γ} (10)	δ_{γ} (11)	$\log L_{\gamma}$ (12)
2FGLJ1058.4+0133	PKS 1055+01	F	0.89	5.12E-09	2.217	0.21	0.93	D01	3.56	6.48	47.10
2FGLJ1058.6+5628	TXS 1055+567	H	0.143	4.79E-09	1.927	2.19	1.76	D01	5.15	2.89	45.30
2FGLJ1103.4-2330	1ES 1101-232	H	0.186	4.90E-10	1.801	10.2	1.03	D01	6.19	4.51	44.64
2FGLJ1104.4+3812	Mkn 421	H	0.03	2.97E-08	1.771	58.4	1.82	D01	6.48	2.77	44.79
2FGLJ1117.2+2013	RBS 0958	H	0.139	1.86E-09	1.702	7.31	0.9	D01	7.22	3.83	45.00
2FGLJ1121.0+4211	RBS 0970	H	0.124	1.17E-09	1.606	1.83	1.62	D01	8.42	2.98	44.76
2FGLJ1130.3-1448	PKS 1127-14	F	1.184	1.80E-09	2.697	0.991	0.03	NED	2.34	17.01	46.95
2FGLJ1136.3+6737	BZB J1136+6737	H	0.134	6.10E-10	1.684	3.23	1.39	D01	7.43	3.25	44.49
2FGLJ1136.7+7009	Mkn 180	H	0.045	1.15E-09	1.74	2.62	1.51	D01	6.8	2.05	43.75
2FGLJ1146.8-3812	PKS 1144-379	F	1.048	1.59E-09	2.312	0.41	1.54	D01	3.21	7.22	46.76
2FGLJ1150.1+2419	B2 1147+24	L	0.2	1.30E-09	2.192	0.3	0.96	D01	3.66	2.40	44.93
2FGLJ1159.5+2914	Ton 599	F	0.724	6.04E-09	2.295	0.44	1.3	D01	3.27	5.63	46.92
2FGLJ1206.0-2638	PKS 1203-26	F	0.789	7.70E-10	2.673	0.443	1.12	NED	2.37	5.91	46.08
2FGLJ1209.6+4121	B3 1206+416	L	0.377	4.30E-10	1.577	0.401	1.1	D01	8.82	4.25	45.39
2FGLJ1217.8+3006	1ES 1215+303	L	0.13	5.49E-09	2.019	0.49	1.88	D01	4.53	2.22	45.22
2FGLJ1221.3+3010	PG 1218+304	H	0.184	2.81E-09	1.709	10.1	1.22	D01	7.14	4.49	45.44
2FGLJ1221.4+2814	W Comae	H	0.102	5.54E-09	2.019	0.4	1.24	D01	4.53	1.91	45.00
2FGLJ1222.4+0413	4C +04.42	F	0.965	1.31E-09	2.766	0.48	0.38	NED	2.24	9.26	46.56
2FGLJ1229.1+0202	3C 273	F	0.158	1.51E-08	2.452	20.4	0.51	D01	2.82	4.75	45.67
2FGLJ1230.2+2517	ON 246	L	0.135	8.80E-10	2.274	0.32	1.89	D01	3.34	1.98	44.35
2FGLJ1248.2+5820	PG 1246+586	L	0.847	4.12E-09	1.949	0.5	1.42	D01	4.99	6.96	47.02
2FGLJ1256.1-0547	3C 279	F	0.536	2.56E-08	2.221	1.34	0.83	D01	3.54	5.99	47.23
2FGLJ1310.6+3222	OP 313	F	0.996	5.30E-09	2.105	0.15	0.99	D01	4.06	6.85	47.26
2FGLJ1315.9-3339	PKS 1313-333	F	1.21	2.57E-09	2.305	0.238	0.35	NED	3.24	10.55	47.14
2FGLJ1337.7-1257	PKS 1335-127	F	0.539	1.77E-09	2.44	0.45	0.63	D01	2.85	5.03	46.03
2FGLJ1408.8-0751	PKS B1406-076	F	1.494	1.74E-09	2.429	0.0828	0.07	NED	2.87	11.93	47.21
2FGLJ1418.1+2539	BZB J1417+2543	H	0.237	4.50E-10	1.98	4.28	1.37	D01	4.78	4.07	44.73
2FGLJ1426.1+3406	BZB J1426+3404	H	1.553	4.90E-10	1.834	0.102	1.5	NED	5.89	9.74	46.77
2FGLJ1428.0-4206	PKS B1424-418	F	1.522	1.47E-08	1.962	0.238	0.29	NED	4.9	14.36	48.20
2FGLJ1428.6+4240	H 1426+428	H	0.129	7.50E-10	1.316	4.64	0.92	D01	13.5	3.76	44.79
2FGLJ1437.1+5640	BZB J1436+5639	H	0.15	4.70E-10	1.533	0.3	1.22	D01	9.48	2.48	44.58
2FGLJ1439.2+3932	PG 1437+398	H	0.344	4.10E-10	1.69	1.19	1.55	D01	7.36	4.49	45.21
2FGLJ1442.7+1159	1ES 1440+122	H	0.163	4.60E-10	1.405	1.22	1.2	D01	11.7	3.34	44.73
2FGLJ1501.0+2238	MS 1458.8+2249	H	0.235	1.89E-09	1.771	0.11	2.31	D01	6.48	2.63	45.46
2FGLJ1504.3+1029	PKS 1502+106	F	1.839	4.01E-08	2.147	0.0583	0.14	NED	3.86	13.77	48.82
2FGLJ1509.7+5556	SBS 1508+561	L	2.025	3.90E-10	1.758	0.05	1.99	D01	6.62	11.16	46.96
2FGLJ1512.8-0906	PKS 1510-08	F	0.36	4.06E-08	2.288	0.49	0.35	D01	3.29	4.03	46.99
2FGLJ1517.7-2421	AP Librae	L	0.049	5.16E-09	2.055	0.62	1.36	D01	4.33	1.54	44.28
2FGLJ1518.0+6526	1H 1515+660	H	0.702	6.90E-10	1.665	7.42	1.29	D01	7.66	9.99	46.17
2FGLJ1522.7-2731	PKS 1519-273	L	1.294	3.55E-09	2.215	0.39	1.03	D01	3.56	9.97	47.36
2FGLJ1549.5+0237	PKS 1546+027	F	0.414	1.82E-09	2.455	0.84	1.18	D01	2.81	4.11	45.74
2FGLJ1550.7+0526	4C +05.64	F	1.422	1.02E-09	2.32	0.202	0.35	NED	3.19	12.15	46.92
2FGLJ1555.7+1111	PG 1553+113	H	0.36	1.40E-08	1.665	13.4	1.85	D01	7.66	6.27	46.81
2FGLJ1613.4+3409	OS 319	F	1.397	4.90E-10	2.307	0.24	0.76	D01	3.23	10.57	46.58
2FGLJ1635.2+3810	4C +38.41	F	1.814	1.16E-08	2.248	0.42	0.53	D01	3.44	17.21	48.26
2FGLJ1653.9+3945	Mkn 501	H	0.034	8.77E-09	1.738	46.4	0.8	D01	6.82	2.83	44.36
2FGLJ1719.3+1744	PKS 1717+177	L	0.137	2.23E-09	1.842	0.48	1.54	D01	5.82	2.37	44.97
2FGLJ1725.0+1151	1H 1720+117	H	0.018	3.70E-09	1.928	3.6	1.65	D01	5.14	1.53	43.31
2FGLJ1728.2+5015	I Zw 187	H	0.055	8.10E-10	1.833	3.63	1.39	D01	5.9	2.22	43.71
2FGLJ1734.3+3858	B2 1732+38A	F	0.97	3.55E-09	2.245	0.05	0.58	D01	3.45	5.76	47.03
2FGLJ1742.1+5948	RGB 1742+597	L	0.4	5.30E-10	2.225	0.03	1.96	D01	3.53	2.51	45.23
2FGLJ1744.1+1934	S3 1741+19	H	0.084	6.30E-10	1.617	1.61	1.1	D01	8.27	2.41	44.11
2FGLJ1748.8+7006	S4 1749+70	L	0.77	2.14E-09	2.04	0.15	1.44	D01	4.41	5.25	46.60
2FGLJ1751.5+0938	OT 081	L	0.322	4.56E-09	2.101	0.76	0.89	D01	4.08	3.81	45.99
2FGLJ1800.5+7829	S5 1803+784	L	0.68	4.45E-09	2.231	0.24	0.45	D01	3.5	5.80	46.73
2FGLJ1806.7+6948	3C 371	L	0.051	3.83E-09	2.189	0.52	0.75	D01	3.67	1.36	44.11
2FGLJ1824.0+5650	4C +56.27	L	0.664	2.63E-09	2.434	0.27	0.96	D01	2.86	5.05	46.43

Table 1 – Continued.

Name (1)	Other name (2)	C (3)	z (4)	F_γ (5)	α_γ (6)	$F_{1 \text{ keV}}$ (7)	α_X (8)	Ref (9)	E_γ (10)	δ_γ (11)	$\log L_\gamma$ (12)
2FGLJ1833.6–2104	PKS 1830–211	F	2.507	1.19E–08	2.462	1.32	0.14	NED	2.79	41.69	48.67
2FGLJ1838.7+4759	GB6 J1838+4802	H	0.3	1.20E–09	1.725	0.1	2.1	D01	6.96	2.96	45.52
2FGLJ 1924.8–2912	PKS B1921–293	F	0.353	3.03E–09	2.432	1.06	0.89	D01	2.87	4.05	45.79
2FGLJ 2000.0+6509	1ES 1959+650	H	0.047	5.88E–09	1.937	9.2	1.68	D01	5.07	2.32	44.35
2FGLJ 2009.5–4850	PKS 2005–489	H	0.071	3.83E–09	1.779	25.4	1.32	D01	6.41	3.30	44.64
2FGLJ 2035.4+1058	PKS 2032+107	L	0.601	1.54E–09	2.552	1.22	1.43	D01	2.59	5.28	46.07
2FGLJ 2056.2–4715	PKS 2052–47	F	1.489	8.63E–09	2.23	0.668	1.77	NED	3.51	10.29	47.91
2FGLJ2133.8–0154	PKS 2131–021	L	1.285	9.50E–10	2.317	0.05	1.05	D01	3.2	6.90	46.77
2FGLJ2148.2+0659	4C +06.69	F	0.99	3.90E–10	2.769	1.85	0.4	NED	2.23	12.45	46.06
2FGLJ2150.2–1412	TXS 2147–144	H	0.229	4.60E–10	2.034	0.736	0.76	NED	4.45	3.14	44.67
2FGLJ2157.9–1501	PKS 2155–152	F	0.672	1.13E–09	2.189	0.22	1.17	D01	3.67	4.97	46.13
2FGLJ2158.8–3013	PKS 2155–304	H	0.116	2.35E–08	1.838	44.9	1.62	D01	5.86	4.15	45.84
2FGLJ2202.8+4216	BL Lacertae	L	0.069	1.05E–08	2.107	2.2	0.83	D01	4.05	2.04	44.85
2FGLJ2203.4+1726	PKS 2201+171	F	1.075	6.53E–09	2.092	0.08	0.41	D01	4.13	7.40	47.44
2FGLJ2211.9+2355	PKS 2209+236	F	1.125	9.70E–10	1.988	0.0464	0.32	NED	4.73	7.12	46.69
2FGLJ2225.6–0454	3C 446	F	1.404	2.23E–09	2.436	0.27	1.09	D01	2.86	9.63	47.24
2FGLJ2229.7–0832	PKS 2227–08	F	1.56	4.27E–09	2.406	0.861	0.35	NED	2.93	18.23	47.65
2FGLJ2232.4+1143	CTA 102	F	1.037	2.88E–09	2.327	0.73	0.51	D01	3.16	10.54	47.00
2FGLJ2243.2–2540	PKS 2240–260	L	0.774	1.62E–09	2.3	0.07	0.79	D01	3.25	4.77	46.42
2FGLJ2250.0+3825	B3 2247+381	H	0.119	1.09E–09	1.837	0.6	1.51	D01	5.87	2.29	44.52
2FGLJ2253.9+1609	3C 454.3	F	0.859	9.65E–08	2.226	1.37	0.62	D01	3.52	9.60	48.33
2FGLJ2258.0–2759	PKS 2255–282	F	0.926	2.87E–09	2.257	0.175	0.38	NED	3.4	7.42	46.88
2FGLJ2322.6+3435	TXS 2320+343	H	0.098	4.30E–10	1.739	0.42	0.8	D01	6.81	1.92	44.00
2FGLJ2347.0+5142	1ES 2344+514	H	0.044	1.55E–09	1.716	5.26	1.13	D01	7.06	2.19	43.84

Notes: Column (1) gives the name of the source in 2FGL; Col. (2) other name for the source; Col. (3) classification (H for HBL, L for LBL and F for FSRQ); Col. (4) the redshift; Col. (5) the γ -ray photons in 1–100 GeV in units of photon cm $^{-2}$ s $^{-1}$ from Ackermann et al. (2011) and Nolan et al. (2012); Col. (6) the photon spectral index from Ackermann et al. (2011) and Nolan et al. (2012); Col. (7) the X-ray flux density in units of μJy at 1 keV; Col. (8) the X-ray spectral index, α ($F_{\nu_X} \propto \nu_X^{-\alpha}$), and Col. (9) reference for Cols. (6) and (7). D01 stands for Donato et al. (2001), the rest are from NED; Col. (10) average γ -ray photon energy, $\langle E_\gamma \rangle$, in units of GeV; Col. (11) the derived lower limit for the γ -ray Doppler factor, δ_γ ; Col. (12) the γ -ray luminosity in erg s $^{-1}$.

2.3 Calculations

For a source, the γ -ray luminosity can be calculated from the detected photons (see Fan et al. 2012b).

$$L_\gamma = 4\pi d_L^2 (1+z)^{(\alpha_{\text{ph}}-2)} f,$$

where d_L is the luminosity distance and f is the integral flux in units of GeV cm $^{-2}$ s $^{-1}$, which can be expressed as

$$f = N_{(E_L \sim E_U)} \left(\frac{1}{E_L} - \frac{1}{E_U} \right) \ln \frac{E_U}{E_L}, \quad \text{if } \alpha_{\text{ph}} = 2, \text{ otherwise}$$

$$f = N_{(E_L \sim E_U)} \frac{1 - \alpha_{\text{ph}}}{2 - \alpha_{\text{ph}}} \frac{(E_U^{2-\alpha_{\text{ph}}} - E_L^{2-\alpha_{\text{ph}}})}{(E_U^{1-\alpha_{\text{ph}}} - E_L^{1-\alpha_{\text{ph}}})}.$$

Here $N_{(E_L \sim E_U)}$ is the number of photons in the energy range of E_L and E_U . In this paper, E_L and E_U correspond to 1 GeV and 100 GeV respectively. The calculated luminosities are listed in Col. (12) of Table 1.

From Table 1, we can derive the average γ -ray luminosity for different subclasses as follows: $\langle \log L_\gamma |^{\text{FSRQs}} \rangle = 47.06 \pm 0.82$ erg s $^{-1}$ for the 54 FSRQs, $\langle \log L_\gamma |^{\text{LBLs}} \rangle = 46.14 \pm 1.01$ erg s $^{-1}$

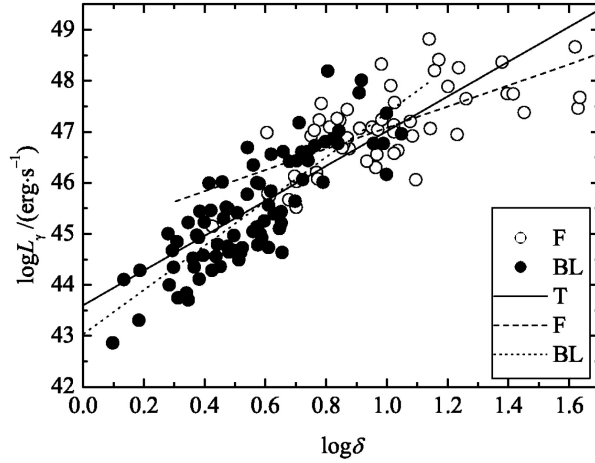


Fig. 1 Plot of the γ -ray luminosity, $\log \nu L_\nu$ (erg s^{-1}), versus the γ -Doppler factor, $\log \delta_\gamma$, for the Fermi blazars. The open circles stand for FSRQs, and the filled points for BLs. The solid line represents the best fitting result for the whole sample, the broken line denotes FSRQs, and the dotted line signifies BLs.

for the 36 LBLS, and $\langle \log L_\gamma |^{\text{HBLs}} \rangle = 44.94 \pm 0.83 \text{ erg s}^{-1}$ for the 48 HBLs. The average values of $\log L_\gamma$ suggest there is a sequence such that $\log L_\gamma |^{\text{FSRQs}} > \log L_\gamma |^{\text{LBLS}} > \log L_\gamma |^{\text{HBLs}}$.

The lower limit of the γ -ray Doppler factor can be obtained from Equation (4) if the redshift, the variability timescale, the X-ray flux density at 1 keV and the γ -ray energy are known. Although the variability timescales are available for a few sources (Yang & Fan 2010), they are not known for most sources. We take one day for the timescale, $\Delta T = 1 \text{ d}$, as in Ghisellini et al. (1998). We use the averaged energy for E_γ , which can be calculated by $\langle E \rangle = \frac{\int E dN}{\int dN}$, and is listed in Col. (10) of Table 1. Therefore, the lower limit of the γ -ray Doppler factor can be estimated and listed in Col. (11) of Table 1.

From the obtained results, we have $\langle \log \delta_\gamma |^{\text{FSRQs}} \rangle = 12.14 \pm 9.38$ for the 54 FSRQs, $\langle \log \delta_\gamma |^{\text{LBLS}} \rangle = 4.64 \pm 2.44$ for the 36 LBLS, and $\langle \log \delta_\gamma |^{\text{HBLs}} \rangle = 3.63 \pm 1.76$ for the 48 HBLs. The average values of $\log \delta_\gamma$ also suggest there is a sequence such that $\delta_\gamma |^{\text{FSRQs}} > \delta_\gamma |^{\text{LBLS}} > \delta_\gamma |^{\text{HBLs}}$.

Based on the calculated γ -ray luminosity and the γ -ray Doppler factors, we can obtain

$$\log L_\gamma (\text{erg s}^{-1}) = (3.41 \pm 0.18) \log \delta + (43.60 \pm 0.14)$$

with a correlation coefficient $r = 0.85$ and a chance probability of $p < 10^{-4}$ for the whole sample (see Fig. 1, see also Fan et al. 2012a). When we consider the subclasses FSRQs and BLs separately, we have

$$\log L_\gamma (\text{erg s}^{-1}) = (2.07 \pm 0.31) \log \delta + (45.00 \pm 0.32)$$

with a correlation coefficient $r = 0.68$ and chance probability of $p < 10^{-4}$ for the 54 FSRQs, and

$$\log L_\gamma (\text{erg s}^{-1}) = (4.34 \pm 0.33) \log \delta + (43.03 \pm 0.19)$$

with a correlation coefficient of $r = 0.83$ and chance probability of $p < 10^{-4}$ for 84 BLs. The corresponding plots are shown in Figure 1.

3 DISCUSSION

Blazars are the subclass of AGNs with special observational properties, which are explained by the relativistic beaming effect. The γ -ray loud blazars detected in highly energetic bands provide us with a good opportunity to investigate the emission mechanism and the beaming effects, as we summarized in our previous paper (Fan et al. 1998). There are several models for the γ -ray emissions. The soft photons are scattered up to the γ -ray region, or the γ -rays are from the synchrotron emissions of ultra-relativistic electrons and positrons produced in a proton-induced cascade (PIC) (Mannheim & Biermann 1992; Mannheim 1993; Cheng & Ding 1994). For the soft photons, there are two main processes: (1) The synchrotron self-Compton model (SSC). In this model, the scattered soft photons are from the synchrotron emissions in the jet (Maraschi et al. 1992; Bloom & Marscher 1996; Zdziarski & Krolik 1993). (2) The inverse Compton process on the external photons (EC), in which the soft photons are either from a nearby accretion disk (Dermer et al. 1992; Coppi et al. 1993), or from disk radiation reprocessed in the broad emission line region of AGNs (Sikora et al. 1994; Blandford & Levinson 1995).

Based on data from the EGRET mission, the beaming effect in the γ -ray regions is discussed. This effect is revisited using the Fermi detected blazars (see Arshakian et al. 2010; Fan et al. 2008; Kovalev et al. 2009; Pushkarev et al. 2010; Savolainen et al. 2010 and Fan et al. 2012b). However, the beaming effect is mostly investigated using the radio emissions (including the radio Doppler factor, δ_R , radio variability and radio polarization). It is possible that the radio Doppler factors, δ_R , are not the same as those in the γ -rays, δ_γ . In this case, the disagreement in the two Doppler factors would result in some false results.

In this paper, based on the proposed model (Mattox et al. 1993, see also von Montigny et al. 1995), we can calculate the lower limit of the γ -ray Doppler factors for the sources with available X-ray and gamma-ray emissions. The calculated results are obtained for 138 blazars (54 FSRQs, 36 LBLs and 48 HBLs) for the case of the variability time scales being one day as in Ghisellini et al. (1998). When the variability time scale is six hours, $\Delta T = 6$ h, the resulting Doppler factor will be a little greater than that obtained for $\Delta T = 24$ h, namely $\delta_{6\text{ h}} \sim 1.4\delta_{24\text{ h}} - 0.70$.

The distance used in this paper is different from that used in Mattox et al. (1993). There are two sources (1633+382 and 3C 279), and their γ -ray Doppler factors were determined in the paper by Mattox and here. We can compare these results.

The quasar 1633+382 is located at $z = 1.8$ and has an X-ray flux density of $F_{1\text{ keV}} = 0.08 \mu\text{Jy}$, with a time scale of two days. When $\alpha_X = 0.7$, $q_0 = 0.5$ and $H_0 = 75 \text{ km Mpc}^{-1} \text{ s}^{-1}$ are adopted, a γ -ray Doppler factor of $\delta_\gamma \geq 7.6$ (for $E_\gamma = 3 \text{ GeV}$) was obtained by Mattox et al. (1993), who used the luminosity distance of $d_L = \frac{100}{H_0} \times 1.85 \times 10^{28} (1+z-\sqrt{1+z}) \text{ cm}$. With those parameters, and using the luminosity distance given by Equation (2) in this work, we then have $\delta_\gamma \geq 8.8$ (for $E_\gamma = 3 \text{ GeV}$). In this work, we adopted the X-ray data, $F_{1\text{ keV}} = 0.42 \mu\text{Jy}$ and $\alpha_X = 0.53$ from Donato et al. (2001) and $\Delta T = 1 \text{ d}$, and obtained a γ -ray Doppler factor of $\delta_\gamma \geq 17.21$ (for $E_\gamma = 3.44 \text{ GeV}$). $\delta_\gamma \geq 15.01$ can be obtained if $\Delta T = 2 \text{ d}$ is adopted.

For 3C 279, Mattox et al. (1993) adopted a time scale of $\Delta T = 2 \text{ d}$ (Kniffen et al. 1993), $\alpha = 0.7$, $h_{75} = 1$, $E_\gamma = 3 \text{ GeV}$ and $F_{\text{keV}} = 0.8 \mu\text{Jy}$, and obtained $\delta_\gamma \geq 3.9$. With those parameters and the luminosity distance Equation (2), we can get $\delta_\gamma \geq 5.1$. In this work, we adopted the X-ray data, $F_{1\text{ keV}} = 1.34 \mu\text{Jy}$ and $\alpha_X = 0.83$ from Donato et al. (2001) and set $\Delta T = 1 \text{ d}$, and we obtained a γ -ray Doppler factor of $\delta_\gamma \geq 7.65$ (for $E_\gamma = 3.54 \text{ GeV}$); $\delta_\gamma \geq 5.3$ can be obtained if $\Delta T = 2 \text{ d}$ is adopted. Our calculation results are consistent with those given in Mattox et al. (1993). However, it is clear that the Doppler factor obtained using the luminosity distance Equation (2) is greater than that obtained using the distance of $d_L = \frac{100}{H_0} \times 1.85 \times 10^{28} (1+z-\sqrt{1+z}) \text{ cm}$ by Mattox et al. (1993). It is clear that the γ -ray Doppler factor determined in this paper using luminosity distance in the Λ -CDM model (Capelo & Natarajan 2007) is greater than that determined in Mattox et al. (1993).

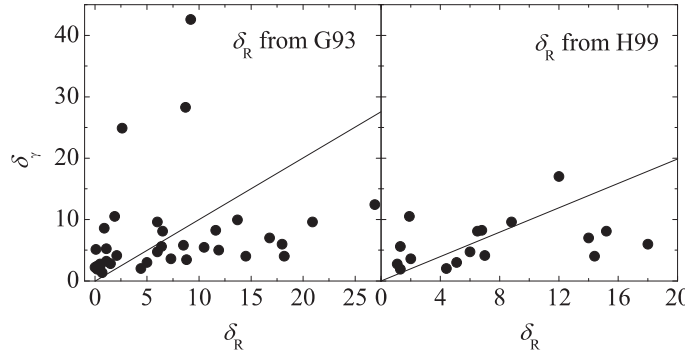


Fig. 2 Plot of the γ -Doppler factor, δ_γ , versus the radio Doppler factor, δ_R , for some Fermi blazars. The radio Doppler factors in the left panel are from Ghisellini et al. (1993), and those in the right panel are from Huang et al. (1999). The solid lines stand for $\delta_\gamma = \delta_R$.

We also compared the obtained γ -ray Doppler factor (δ_γ) with the radio Doppler factor (δ_R). Some methods are proposed to estimate the Doppler factor: (i) the Doppler factor (δ_{SSC}) can be derived by a synchrotron self-Compton (SSC) model (see Ghisellini et al. 1993); (ii) the Doppler factor (δ_{eq}) can be estimated using single-epoch radio data by assuming that the sources have an equipartition of energy between radiating particles and the magnetic field (Readhead 1994); and (iii) the Doppler factor (δ_{var}) can be estimated using the radio flux density variations (Lähteenmäki & Valtaoja 1999). Furthermore, the lower limits of the Doppler factor have been estimated for the γ -ray loud blazars (Dondi & Ghisellini 1995; Cheng et al. 1999; Fan 2005; Fan et al. 1999; Ghisellini et al. 1998).

For the radio Doppler factors estimated using the SSC model (Ghisellini et al. 1993; Huang et al. 1999), we compiled the relevant data and listed them in Table 2. The corresponding plot of the γ -ray Doppler factor versus the radio Doppler factor is shown in Figure 2. In the left panel of Figure 2, we can see that, except for the three points in the top left corner, the estimated γ -ray Doppler factors are not correlated with the radio Doppler factors.

For the radio Doppler factors estimated from the variability (or brightness temperature), we have compiled them from the literature (Lähteenmäki & Valtaoja 1999; Fan et al. 2009; Hovatta et al. 2009) and listed them in Table 3.

It is clear that for some sources, their radio Doppler factors are available in three papers, some are in two papers, while the rest are only obtained in one paper. Therefore, we used the averaged value of the radio Doppler factor if more than one radio Doppler factor is available when compared with the γ -ray Doppler factor. The result is shown in Figure 3, which suggests that there is a tendency for the γ -ray Doppler factor to increase with the radio Doppler factor.

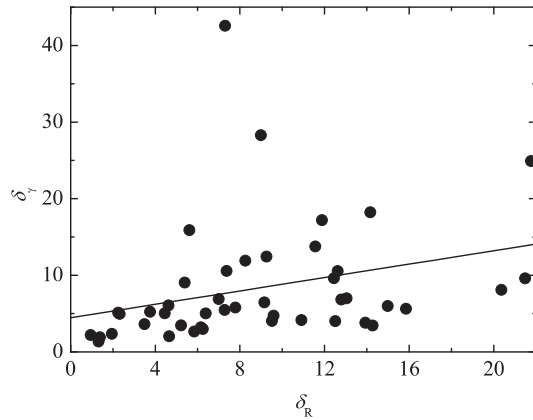
For the Doppler factors estimated from the SSC model and the variability (or brightness temperature), we found that the γ -ray Doppler factors are more consistent with the Doppler factors estimated in the latter method than with those estimated in the former method. Does that mean the Doppler factors estimated from the variability are more reliable? This is worthy of discussion using a larger sample with available radio Doppler factors.

The γ -ray Doppler factors were also estimated by Zeng & Zhang (2011) using the dependence of the Doppler factor on the frequency (see Fan et al. 1993; Zhang et al. 2002). In the work by Zeng & Zhang (2011), the γ -ray Doppler factors are strongly correlated with the radio Doppler factors. In our analysis, except for the two points (1ES 0212+735, $\delta_\gamma = 42.59$, and 4C +71.07, $\delta_\gamma = 28.29$), other points in Figure 2 follow a close correlation between the γ -ray Doppler factor and the radio

Table 2 γ -ray and Radio Doppler Factors for some Fermi Blazars

Name (1)	δ_R^{G93} (2)	δ_R^{H99} (3)	δ_γ (4)	Name (5)	δ_R^{G93} (6)	δ_R^{H99} (7)	δ_γ (8)
PKS 0048–09	10.5	—	5.47	Ton 599	6.4	1.3	5.63
PKS 0208–512	—	15.2	8.12	1ES 1215+303	0.4	—	2.22
S5 0212+73	9.2	—	42.59	W Comae	0.2	1.3	1.91
3C 66A	0.1	—	5.14	3C 273	6	6	4.75
AO 0235+164	6.5	6.5	8.11	3C 279	18	18	5.99
PKS 0420–01	16.8	14	7.01	PKS 1335–127	11.9	—	5.03
PKS 0528+134	2.6	—	24.91	PKS 1510–08	14.5	14.4	4.03
PKS 0537–441	11.6	6.8	8.25	PKS 1519–273	13.7	—	9.97
S5 0716+71	2.1	7	4.16	Mkn 501	1.5	—	2.83
PKS 0735+17	7.3	2	3.63	I Zw 187	0.01	—	2.22
PKS 0754+100	1.1	—	3.22	S4 1749+70	1.1	—	5.25
PKS 0829+046	0.2	—	2.42	S5 1803+784	8.5	—	5.80
4C +71.07	8.7	—	28.29	3C 371	0.7	—	1.36
OJ 287	8.8	—	3.46	PKS B1921–293	18.2	—	4.05
S4 0954+65	5	5.1	3.00	4C +06.69	26.9	—	12.45
S5 1039+81	0.9	—	8.59	BL Lacertae	4.4	4.4	2.04
Mkn 421	0.5	1.1	2.77	3C 446	20.9	—	9.63
PKS 1127–14	—	12	17.01	CTA 102	1.9	1.9	10.54
B2 1147+24	0.5	—	2.40	3C 454.3	6	8.8	9.60

Notes: G93 – Ghisellini et al. 1993; H99 – Huang et al. (1999). Columns (1) and (5) list the name of the source; Cols. (2) and (6) give the radio Doppler factors from Ghisellini et al. (1993); Cols. (3) and (7) show the radio Doppler factors from Huang et al. (1999), and Cols. (4) and (8) contain the γ -ray Doppler factor obtained in this work.

**Fig. 3** Plot of the γ -Doppler factor, δ_γ , versus the radio Doppler factor, δ_R , for some Fermi blazars.

Doppler factor. It may be that the time scale of one day is too short for 1ES 0212+735 and 4C +71.07. In this sense, it is possible to use the radio Doppler factor to replace the γ -ray Doppler factor in discussions of the beaming effect for Fermi loud blazars.

In this work, the lower limits of the γ -ray Doppler factors are estimated for a sample of 138 Fermi loud blazars with available X-ray observations. For some sources, the γ -ray Doppler factors are compared with the available radio Doppler factor and found to show a tendency for the γ -ray Doppler factors to increase with the radio Doppler factors. The analysis based on the presently

Table 3 γ -ray and Radio Doppler Factors for some Fermi Blazars

Name (1)	δ_R^{F09} (2)	δ_R^{H09} (3)	δ_R^{L99} (4)	δ_γ (5)	Name (6)	δ_R^{F09} (7)	δ_R^{H09} (8)	δ_R^{L99} (9)	δ_γ (10)
PKS 0048–09	4.97	9.6	–	5.47	B2 1308+32	11.58	15.4	11.38	6.85
1ES 0212+735	9.23	8.5	4.16	42.59	PKS 1335–127	6.38	–	–	5.03
PKS 0215+015	5.61	–	–	15.9	PKS 1406–076	–	–	8.26	11.93
3C 66A	–	2.6	1.99	5.14	PKS 1502+106	–	12	11.13	13.77
PKS 0235+164	20.74	24	16.32	8.11	PKS 1510–08	7.64	16.7	13.18	4.03
PKS 0420–01	7.49	19.9	11.72	7.01	B2 1611+34	3.36	13.7	5.04	10.57
PKS 0528+134	19.84	31.2	14.22	24.91	B3 1633+382	5.29	21.5	8.83	17.21
S5 0716+714	–	10.9	–	4.16	PKS 1717+177	1.94	–	–	2.37
PKS 0735+17	–	3.8	3.17	3.63	S5 1749+701	3.75	–	–	5.25
PKS 0736+01	–	8.6	3.08	2.66	4C +09.57	–	12	15.85	3.81
PKS 0754+100	7.33	5.6	5.52	3.22	8C 1803+784	4.7	12.2	6.45	5.8
PKS 0808+019	5.39	–	–	9.04	3C 371	1.05	1.1	1.8	1.36
B3 0814+425	–	4.6	5.84	3.48	4C +56.27	2.5	6.4	–	5.05
4C +71.07	–	16.3	10.67	28.29	PKS B1921–293	9.51	–	–	4.05
OJ 287	7.76	17	18.03	3.46	4C 02.81	7	–	–	6.9
S4 0954+55	–	–	4.63	6.09	4C +06.69	4.35	15.6	7.81	12.45
S4 0954+65	5.93	6.2	6.62	3	PKS 2155–152	2.31	–	–	4.97
PKS 1055+01	7.49	12.2	7.78	6.48	BL Lac	2.77	7.3	3.91	2.04
4C +29.45	9.63	28.5	9.42	5.63	3C 446	9.93	16	11.38	9.63
B2 1215+30	0.94	–	–	2.22	PKS 2227–08	–	15.9	12.42	18.23
1219+285	–	1.2	1.56	1.91	CTA 102	8.02	15.6	14.23	10.54
3C 273	6.05	17	5.71	4.75	3C 454.3	9.38	33.2	21.84	9.6
3C 279	4.16	24	16.77	5.99					

Notes: F09 – Fan et al. (2009); H09 – Hovatta et al. (2009); L99 – Lähteenmäki & Valtaoja (1999). Columns (1) and (6) give the name of the source; Cols. (2) and (7) list the radio Doppler factors from Fan et al. (2009); Cols. (3) and (8) show the radio Doppler factors from Hovatta et al. (2009); Cols. (4) and (9) contain the radio Doppler factors from Lähteenmäki & Valtaoja (1999), and Cols. (5) and (10) represent the γ -ray Doppler factors obtained in this work.

available radio Doppler factors suggests that the radio Doppler factors estimated from the variability can be used to discuss the beaming effect in the Fermi loud blazars.

Acknowledgements The work is partially supported by the National Natural Science Foundation of China (Grant No. 11173009), the National Basic Research Program of China (973 program, 2007CB815405) and the Bureau of Education of Guangzhou Municipality (No.11 Sui-Jiao-Ke[2009]), Guangdong Province Universities and Colleges Pearl River Scholar Funded Scheme (GDUPS) (2009), Yangcheng Scholar Funded Scheme (10A027S), and the Joint Laboratory for Optical Astronomy of Chinese Academy of Sciences.

References

- Abdo, A. A., Ackermann, M., Ajello, M., et al. 2009, ApJ, 700, 597
- Abdo, A. A., Ackermann, M., Ajello, M., et al. 2010, ApJS, 188, 405
- Ackermann, M., Ajello, M., Allafort, A., et al. 2011, ApJ, 743, 171
- Aller, M. F., Aller, H. D., & Hughes, P. A. 2011, Journal of Astrophysics and Astronomy, 32, 5
- Arshakian, T. G., León-Tavares, J., Torrealba, J., & Chavushyan, V. H. 2010, arXiv:1006.2079
- Bastieri, D., Ciprini, S., & Gasparrini, D. 2011, Journal of Astrophysics and Astronomy, 32, 169
- Blandford, R. D., & Levinson, A. 1995, ApJ, 441, 79
- Bloom, S. D., & Marscher, A. P. 1996, ApJ, 461, 657
- Capelo, P. R., & Natarajan, P. 2007, New Journal of Physics, 9, 445

- Cheng, K. S., & Ding, W. K. Y. 1994, A&A, 288, 97
- Cheng, K. S., Fan, J. H., & Zhang, L. 1999, A&A, 352, 32
- Coppi, P. S., Kartje, J. F., & Königl, A. 1993, in American Institute of Physics Conference Series, 280, eds. M. Friedlander, N. Gehrels, & D. J. Macomb, 559
- Dermer, C. D., Schlickeiser, R., & Mastichiadis, A. 1992, A&A, 256, L27
- Donato, D., Ghisellini, G., Tagliaferri, G., & Fossati, G. 2001, A&A, 375, 739
- Dondi, L., & Ghisellini, G. 1995, MNRAS, 273, 583
- Fan, J. H. 2005, A&A, 436, 799
- Fan, J. H., Xie, G. Z., Li, J. J., et al. 1993, ApJ, 415, 113
- Fan, J. H., Xie, G. Z., & Wen, S. L. 1996, A&AS, 116, 409
- Fan, J. H., Adam, G., Xie, G. Z., et al. 1998, A&A, 338, 27
- Fan, J. H., Xie, G. Z., & Bacon, R. 1999, A&AS, 136, 13
- Fan, J.-H., Yuan, Y.-H., Liu, Y., et al. 2008, PASJ, 60, 707
- Fan, J.-H., Huang, Y., He, T.-M., et al. 2009, PASJ, 61, 639
- Fan, J. H., Liu, Y., Li, Y., et al. 2011, Journal of Astrophysics and Astronomy, 32, 67
- Fan, J. H., Yang, J. H., & Liu, Y. 2012a, in IAUS 290 Proceedings, eds. C. M. Zhang, T. Belloni, M. Méndez, & S. N. Zhang, in press
- Fan, J. H., Yang, J. H., Zhang, J. Y., et al. 2012b, arXiv:1210.4096
- Ghisellini, G., Padovani, P., Celotti, A., & Maraschi, L. 1993, ApJ, 407, 65
- Ghisellini, G., Celotti, A., Fossati, G., Maraschi, L., & Comastri, A. 1998, MNRAS, 301, 451
- Ghisellini, G., Tavecchio, F., Foschini, L., et al. 2010, MNRAS, 402, 497
- Gupta, A. C. 2011, Journal of Astrophysics and Astronomy, 32, 155
- Hovatta, T., Valtaoja, E., Tornikoski, M., & Lähteenmäki, A. 2009, A&A, 494, 527
- Huang, L. H., Jiang, D. R., & Cao, X. 1999, A&A, 341, 74
- Kniffen, D. A., Bertsch, D. L., Fichtel, C. E., et al. 1993, ApJ, 411, 133
- Kovalev, Y. Y., Aller, H. D., Aller, M. F., et al. 2009, ApJ, 696, L17
- Lähteenmäki, A., & Valtaoja, E. 1999, ApJ, 521, 493
- Lott, B. 2010, International Journal of Modern Physics D, 19, 831
- Mannheim, K. 1993, Phys. Rev. D, 48, 2408
- Mannheim, K., & Biermann, P. L. 1992, A&A, 253, L21
- Maraschi, L., Ghisellini, G., & Celotti, A. 1992, ApJ, 397, L5
- Marscher, A., Jorstad, S. G., Larionov, V. M., et al. 2011, Journal of Astrophysics and Astronomy, 32, 233
- Mattox, J. R., Bertsch, D. L., Chiang, J., et al. 1993, ApJ, 410, 609
- Nieppola, E., Tornikoski, M., & Valtaoja, E. 2006, A&A, 445, 441
- Nolan, P. L., Abdo, A. A., Ackermann, M., et al. 2012, ApJS, 199, 31
- Pushkarev, A. B., Kovalev, Y. Y., & Lister, M. L. 2010, ApJ, 722, L7
- Readhead, A. C. S. 1994, ApJ, 426, 51
- Romero, G. E., Cellone, S. A., Combi, J. A., & Andruchow, I. 2002, A&A, 390, 431
- Savolainen, T., Homan, D. C., Hovatta, T., et al. 2010, A&A, 512, A24
- Sikora, M., Begelman, M. C., & Rees, M. J. 1994, ApJ, 421, 153
- Urry, M. 2011, Journal of Astrophysics and Astronomy, 32, 139
- Urry, M., & Padovani, P. 1995, PASP, 107, 715
- von Montigny, C., Bertsch, D. L., Chiang, J., et al. 1995, ApJ, 440, 525
- Wills, B. J., Wills, D., Breger, M., Antonucci, R. R. J., & Barvainis, R. 1992, ApJ, 398, 454
- Yang, J., & Fan, J. 2010, Science in China G: Physics and Astronomy, 53, 1921
- Zdziarski, A. A., & Krolik, J. H. 1993, ApJ, 409, L33
- Zeng, H.-D., & Zhang, L. 2011, RAA (Research in Astronomy and Astrophysics), 11, 391
- Zhang, L. Z., Fan, J.-H., & Cheng, K.-S. 2002, PASJ, 54, 159